

Critical stability of few-body systems

V.A. Karmanov^a and J. Carbonell^b

^aLebedev Physical Institute, Moscow, Russia

^bInstitut de Physique Nucleaire, Orsay, France

February 27, 2022

Abstract

When a two-body system is bound by a zero-range interaction, the corresponding three-body system – considered in a non-relativistic framework – collapses, that is its binding energy is unbounded from below. In a paper by J.V. Lindesay and H.P. Noyes [1] it was shown that the relativistic effects result in an effective repulsion in such a way that three-body binding energy remains also finite, thus preventing the three-body system from collapse. Later, this property was confirmed in other works based on different versions of relativistic approaches. However, the three-body system exists only for a limited range of two-body binding energy values. For stronger two-body interaction, the relativistic three-body system still collapses.

A similar phenomenon was found in a two-body systems themselves: a two-fermion system with one-boson exchange interaction in a state with zero angular momentum $J = 0$ exists if the coupling constant does not exceed some critical value but it also collapses for larger coupling constant. For a $J = 1$ state, it collapses for any coupling constant value. These properties are called "critical stability". This contribution aims to be a brief review of this field pioneered by H.P. Noyes.

1 Introduction

The radius of nuclear forces – the interaction between protons and neutrons – is sensibly smaller than the size of nuclei themselves. Since the wave function at large distances r behaves as $\sim \exp(-|E_b|r)$, the latter is determined by the nuclear binding energy E_b . The binding energy, in its turn, is a cancellation of a large (negative) potential energy and large (positive) kinetic energy. Therefore E_b is much smaller than each of these energies and the nuclear radius $r \sim 1/|E_b|$ can be larger than the radius of the nuclear forces. To understand qualitatively some nuclear properties, one can consider the "zero-range interaction limit". To this aim, we approximate the nuclear interaction V by a potential well:

$$V(r) = \begin{cases} -U_0, & \text{if } r < a \\ 0, & \text{if } r > a \end{cases}$$

As it is well known from standard quantum mechanics textbooks (see e.g. [2]), a bound state exists if some relation between the potential depth U_0 and its range a is fulfilled, that is if

$$U_0 > \frac{\pi^2 \hbar^2}{8ma^2}$$

\hbar being the Plank constant and m the mass of the particle. If we let a tend to zero and U_0 to infinity, keeping constant the product $U_0 a^2$, we will get in this limit an infinitely deep zero range potential well, in which a two-body bound state exists.

The zero-range two-body interaction provides an important limiting case which qualitatively reflects characteristic properties of nuclear [3] and atomic [4] few-body systems. It turned out, however, that when using non-relativistic dynamics, it generates the Thomas collapse [5] of the three-body system. The latter means that the three-body binding energy tends to $-\infty$, when the interaction radius tends to zero keeping constant the product $U_0 a^2$ and consequently the two-body binding energy. As an illustration, we have solved numerically the three-body Faddeev equation in momentum space with the two-body amplitude for zero-range interaction as input. The corresponding three-body binding energy is kept finite by introducing a momentum cutoff L . The result for the three-body binding energy (in units of the particle mass m) is shown in fig. 1. We see that when cutoff L is removed (L tends to infinity), the three-body binding energy $|E_3|$ increases monotonously without any limit. This is just the manifestation of the Thomas collapse. Several ways to regularize this interaction have been proposed in the literature [6, 7].

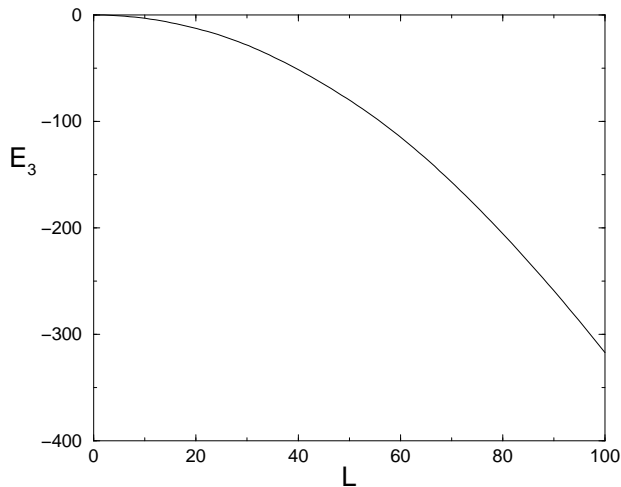


Figure 1: Three-body binding energy (in the units of mass m), for the zero-range two-body interaction and finite two-body binding energy, as a function of momentum cutoff L in the Faddeev equation.

It should be emphasized that the Thomas collapse was found in the non-relativistic framework, which should be applied only when the binding energy is much smaller than the particle mass. We see that the results displayed in fig. 1 do not correspond to this situation: the module of the binding energy $|E_3|$ becomes much larger than particle mass. For example, for the

cutoff $L \approx 50 m$ the binding energy is $E_3 \approx -100 m$. This is far beyond the domain where the non-relativistic treatment is valid. The answer to the question: "what happens with the three-body system in the limit of two-body zero-range interaction" should be obtained in a relativistic framework only.

This answer was first found in the paper by J.V. Lindesay and H.P. Noyes [1] in the so called "minimal relativistic model". It was shown that the relativistic effects result in an effective repulsion and can thus prevent the three-body system from collapse: the three-body binding energy remains also finite.

Later, this property was confirmed in other works based on different versions of relativistic approaches. In particular, two-body calculations showed that in the scalar case, relativistic effects were indeed strongly repulsive [8]. However, it was found [9] that this stabilization had some restrictions: the three-body system exists only in a limited range of two-body binding energy. For stronger two-body interaction, the mass squared of three-body system M_3^2 though remaining finite, crosses zero and becomes negative. This means that the relativistic three-body system does not longer exists. Then a similar phenomenon was also found in the two-body systems: the two-fermion systems with one-boson exchange interaction also collapses if the coupling constant exceeds some critical value. These properties are called "critical stability" and they are forming now an interesting field of research. In what follows we will give a brief review of this developing field pioneered by H.P. Noyes.

2 Relativistic three-body system with zero-range interaction

In paper [1], relativistic three-body calculations with zero-range interaction have been performed in a minimal relativistic model. Later, a much more general and sophisticated approach to the relativistic few-body systems – Light-Front Dynamics – was developed (see for review [10, 11]). In the framework of this relativistic approach the problem of three equal mass (m) bosons interacting via zero-range forces was reconsidered in the [9].

The relativistic three-body equation is derived in Section 2.1. In Section 2.2, their solutions are presented and some concluding remarks are given in Section 4.

2.1 Equation

Our starting point is the explicitly covariant formulation of the Light-Front Dynamics [10]. In non-relativistic approach the wave function $\psi(\vec{r}, t)$ is a probability amplitude defined at a given time t , say at $t = 0$. In four-dimensional Minkowski space one can define the wave function on any space-like plane to preserve the causality, or more generally on any space-like surface. The orientation of this plane is defined by a four-vector $\lambda = (\lambda_0, \vec{\lambda})$ orthogonal to this plane. We can change its orientation moving λ within the light cone in such a way that the plane where the wave function is defined remains space-like. Its limiting value is reached when λ lies on the light-cone surface. Then such the four-vector is denoted by $\omega = (\omega_0, \vec{\omega})$ and has the property $\omega^2 = \omega_0^2 - \vec{\omega}^2 = 0$.

The corresponding plane is given by the equation $\omega \cdot x = 0$. In the particular case $\omega = (1, 0, 0, -1)$ it turns into $t + z = 0$, setting hereafter $c = 1$. This equation coincides with the

light-front equation and therefore the plane $t + z = 0$ is called the light-front plane. The dynamics determining the evolution of the wave function from one light-front plane to another one is the light-front dynamics. This approach was proposed by Dirac [12] and it has many advantages. Later, its explicitly covariant version was developed, when the light-front plane is defined by the covariant equation $\omega \cdot x = 0$ and no any particular axes like t or z is selected [10]. We will just use the light-front dynamics as a relativistic approach.

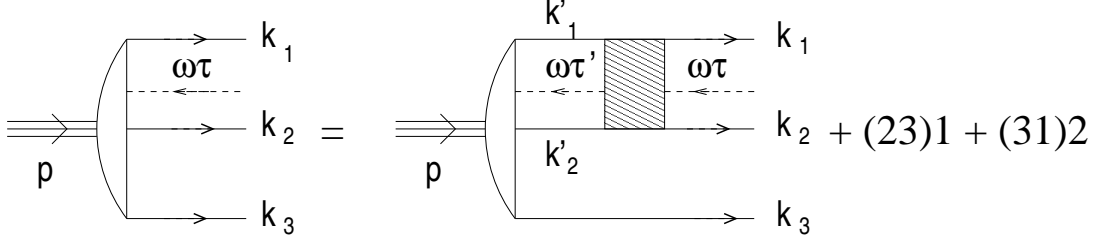


Figure 2: Three-body equation for the vertex function Γ .

The three-body equation is represented graphically in figure 2. It concerns the vertex function Γ , related to the wave function ψ in the standard way:

$$\psi(k_1, k_2, k_3, p, \omega\tau) = \frac{\Gamma(k_1, k_2, k_3, p, \omega\tau)}{\mathcal{M}^2 - M_3^2}, \quad \mathcal{M}^2 = (k_1 + k_2 + k_3)^2 = (p + \omega\tau)^2.$$

All four-momenta are on the corresponding mass shells ($k_i^2 = m^2$, $p^2 = M_3^2$, $(\omega\tau)^2 = 0$) and satisfy the conservation law $k_1 + k_2 + k_3 = p + \omega\tau$ involving $\omega\tau$. The four-momenta $\omega\tau$ and $\omega\tau'$ are drawn in figure 2 by dash lines. The off-energy shell character of the wave function is ensured by non-zero value of the scalar variable τ . In the standard approach [11], the minus-components of the momenta are not conserved and the only non-zero component of ω is $\omega_- = \omega_0 - \omega_z = 2$. Variable 2τ is just the non-zero difference of non-conserved components $2\tau = k_{1-} + k_{2-} + k_{3-} - p_-$.

Applying to figure 2 the covariant light-front graph techniques [10], we find the equation:

$$\begin{aligned} \Gamma(k_1, k_2, k_3, p, \omega\tau) &= \frac{\lambda}{(2\pi)^3} \int \frac{d\tau'}{\tau'} \frac{d^3 k'_1}{2\varepsilon_{k'_1}} \frac{d^3 k'_2}{2\varepsilon_{k'_2}} \Gamma(k'_1, k'_2, k_3, p, \omega\tau') \\ &\times \delta^{(4)}(k'_1 + k'_2 - \omega\tau' - k_1 - k_2 + \omega\tau) + (23)1 + (31)2, \end{aligned} \quad (1)$$

where $\varepsilon_k = \sqrt{m^2 + \vec{k}^2}$. For the zero-range forces we are interested in, the interaction kernel appears as a constant λ . In (1) the contribution of interacting pair (12) is explicitly written while the contributions of the remaining pairs are simply denoted by (23)1 + (31)2.

Equation (1) can be rewritten in variables $\vec{R}_{i\perp}, x_i$, ($i = 1, 2, 3$), where $\vec{R}_{i\perp}$ is the spatial component of the four-vector $R_i = k_i - x_i p$ orthogonal to $\vec{\omega}$ and $x_i = \frac{\omega \cdot k_i}{\omega \cdot p}$ [10]. For this aim we insert in r.h.-side of (1) the unity integral

$$1 = \int 2(\omega \cdot k'_3) \delta^{(4)}(k'_3 - k_3 - \omega\tau_3) d\tau_3 \frac{d^3 k'_3}{2\varepsilon_{k'_3}}$$

and recover the usual three-body space volume which, expressed in the variables $(\vec{R}_{i\perp}, x_i)$, reads

$$\int \delta^{(4)}(\sum_{i=1}^3 k'_i - p - \omega\tau') \prod_{i=1}^3 \frac{d^3 k'_i}{2\varepsilon_{k'_i}} 2(\omega \cdot p) d\tau' = \int \delta^{(2)}(\sum_{i=1}^3 \vec{R}'_{\perp i}) \delta(\sum_{i=1}^3 x'_i - 1) 2 \prod_{i=1}^3 \frac{d^2 R'_{\perp i} dx'_i}{2x'_i}.$$

The Faddeev amplitudes Γ_{ij} are introduced in the standard way:

$$\Gamma(1, 2, 3) = \Gamma_{12}(1, 2, 3) + \Gamma_{23}(1, 2, 3) + \Gamma_{31}(1, 2, 3),$$

and equation (1) is equivalent to a system of three coupled equations for these components. With the symmetry relations $\Gamma_{23}(1, 2, 3) = \Gamma_{12}(2, 3, 1)$ and $\Gamma_{31}(1, 2, 3) = \Gamma_{12}(3, 1, 2)$, the system is reduced to a single equation for one of the amplitudes, say Γ_{12} .

In general, Γ_{12} depends on all variables $(\vec{R}_{i\perp}, x_i)$, constrained by the relations $\vec{R}_{1\perp} + \vec{R}_{2\perp} + \vec{R}_{3\perp} = 0$, $x_1 + x_2 + x_3 = 1$, but for a contact kernel it depends only on $(\vec{R}_{3\perp}, x_3)$ [13]. Equation (1) results into:

$$\Gamma_{12}(\vec{R}_{\perp}, x) = \frac{\lambda}{(2\pi)^3} \int \left[\Gamma_{12}(\vec{R}_{\perp}, x) + 2\Gamma_{12}(\vec{R}'_{\perp} - x'\vec{R}_{\perp}, x'(1-x)) \right] \frac{1}{s'_{12} - M_{12}^2} \frac{d^2 R'_{\perp} dx'}{2x'(1-x')}, \quad (2)$$

in which

$$s'_{12} = (k'_1 + k'_2)^2 = \frac{R'^2_{\perp} + m^2}{x'(1-x')}$$

is the effective on shell mass squared of the two-body subsystem, whereas $M_{12}^2 = (k'_1 + k'_2 - \omega\tau')^2 = (p - k_3)^2$ corresponds to its off-shell mass. It is expressed through M_3^2, R_{\perp}^2, x as

$$M_{12}^2 = (1-x)M_3^2 - \frac{R_{\perp}^2 + (1-x)m^2}{x}. \quad (3)$$

These on- and off-shell masses s'_{12} and M_{12}^2 differ from each other, since $k'_1 + k'_2 + k_3 \neq p$. On the energy shell, at $\tau' = 0$, the value M_{12}^2 turns into s'_{12} , what is never reached for a bound state problem.

Since the first term $\Gamma_{12}(\vec{R}_{\perp}, x)$ in the integrand does not depend on the integration variables \vec{R}'_{\perp}, x' , we can transform (2) as:

$$\Gamma_{12}(\vec{R}_{\perp}, x) = \frac{1}{\lambda^{-1} - I(M_{12})} \frac{2}{(2\pi)^3} \int \Gamma_{12}(\vec{R}'_{\perp} - x'\vec{R}_{\perp}, x'(1-x)) \frac{1}{s'_{12} - M_{12}^2} \frac{d^2 R'_{\perp} dx'}{2x'(1-x')}, \quad (4)$$

where

$$I(M_{12}) = \frac{1}{(2\pi)^3} \int \frac{1}{s'_{12} - M_{12}^2} \frac{d^2 R'_{\perp} dx'}{2x'(1-x')}. \quad (5)$$

The integral (5) diverges logarithmically and we implicitly assume that a cutoff L is introduced.

The value of λ is found by solving the two-body problem with the same zero-range interaction under the condition that the two-body bound state mass has a fixed value M_2 . From that we get $\lambda^{-1} = I(M_2)$ with I given by (5). It also diverges when the momentum space cutoff L tends to infinity (or, equivalently, the interaction range tends to zero). However, the difference $\lambda^{-1} - I(M_{12}) = I(M_2) - I(M_{12})$ which appears in (4) converges in the limit $L \rightarrow \infty$. The factor $F(M_{12}) = 1/[I(M_2) - I(M_{12})]$ gives the two-body off-shell scattering amplitude,

depending on the off-shell two-body mass M_{12} , without any regularization. For $0 \leq M_{12}^2 < 4m^2$ explicit calculations gives:

$$F(M_{12}) = \frac{8\pi^2}{\frac{\arctan y_{M_{12}}}{y_{M_{12}}} - \frac{\arctan y_{M_2}}{y_{M_2}}},$$

where $y_{M_{12}} = \frac{M_{12}}{\sqrt{4m^2 - M_{12}^2}}$ and similarly for y_{M_2} . If $M_{12}^2 < 0$, the amplitude obtains the form:

$$F(M_{12}) = \frac{8\pi^2}{\frac{1}{2y'_{M_{12}}} \log \frac{1 + y'_{M_{12}}}{1 - y'_{M_{12}}} - \frac{\arctan y_{M_2}}{y_{M_2}}},$$

where $y'_{M_{12}} = \frac{\sqrt{-M_{12}^2}}{\sqrt{4m^2 - M_{12}^2}}$.

Finally, the equation for the Faddeev amplitude reads:

$$\Gamma_{12}(R_{\perp}, x) = F(M_{12}) \frac{1}{(2\pi)^3} \int_0^1 dx' \int_0^\infty \frac{\Gamma_{12}(R'_{\perp}, x'(1-x)) d^2 R'_{\perp}}{(\vec{R}'_{\perp} - x' \vec{R}_{\perp})^2 + m^2 - x'(1-x')M_{12}^2}. \quad (6)$$

The three-body mass M_3 enters in this equation through the variable M_{12}^2 , defined by (3).

By replacing $x'(1-x) \rightarrow x'$, equation (6) can be transformed into

$$\Gamma_{12}(R_{\perp}, x) = F(M_{12}) \frac{1}{(2\pi)^3} \int_0^{1-x} \frac{dx'}{x'(1-x-x')} \int_0^\infty \frac{d^2 R'_{\perp}}{\mathcal{M}'^2 - M_3^2} \Gamma_{12}(R'_{\perp}, x'), \quad (7)$$

with

$$\mathcal{M}'^2 = \frac{\vec{R}'_{\perp}{}^2 + m^2}{x'} + \frac{\vec{R}_{\perp}^2 + m^2}{x} + \frac{(\vec{R}'_{\perp} + \vec{R}_{\perp})^2 + m^2}{1-x-x'}$$

This equation is the same than the equation (11) from [13] except for the integration limits of (\vec{R}'_{\perp}, x') variables. In [13] the integration limits follow from the condition $M_{12}^2 > 0$. They read

$$\int_{\frac{m^2}{M_3^2}}^{1-x} [\dots] dx' \int_0^{k_{\perp}^{max}} [\dots] d^2 R'_{\perp} \quad (8)$$

with $k_{\perp}^{max} = \sqrt{(1-x')(M_3^2 x' - m^2)}$ and thus implicitly introduce a lower bound on the three-body mass $M_3 > \sqrt{2}m$. The same condition, though in a different relativistic approach, was used in [1]. The integration limits in (8) restrict the arguments of Γ_{12} to the domain

$$\frac{m^2}{M_3^2} \leq x \leq 1 - \frac{m^2}{M_3^2}, \quad 0 \leq R_{\perp} \leq k_{\perp}^{max}$$

and can be considered as a method of regularization. In this case, one no longer deals with the zero-range forces.

Being interested in studying the zero-range interaction, we do not cut off the variation domain of variables R_{\perp}, x :

$$0 \leq x \leq 1, \quad 0 \leq R_{\perp} < \infty$$

The integration limits for these variables reflect the conservation law of the four-momenta in the three-body system and they are automatically fulfilled, as far as the $\delta^{(4)}$ -function in (1) is taken into account. The off-shell variable M_{12}^2 may take negative values, when R_\perp and x vary in their proper limits. Thus, if $M_3^2 > m^2$ one has $-\infty \leq M_{12}^2 \leq (M_3 - m)^2$ but if $M_3^2 < m^2$, M_{12}^2 is always negative $-\infty \leq M_{12}^2 \leq 0$.

We would like to notice that M_{12}^2 is not to be confused with the on-shell effective mass squared $s'_{12} = (k'_1 + k'_2)^2$ which is indeed always positive and even $s'_{12} \geq 4m^2$. As we will see in the next section, this point turns out to be crucial for the appearance of the relativistic collapse.

2.2 Results

The results of solving equation (6) are presented in what follows. Calculations were carried out with constituent mass $m = 1$ and correspond to the ground state. We represent in fig. 3a the

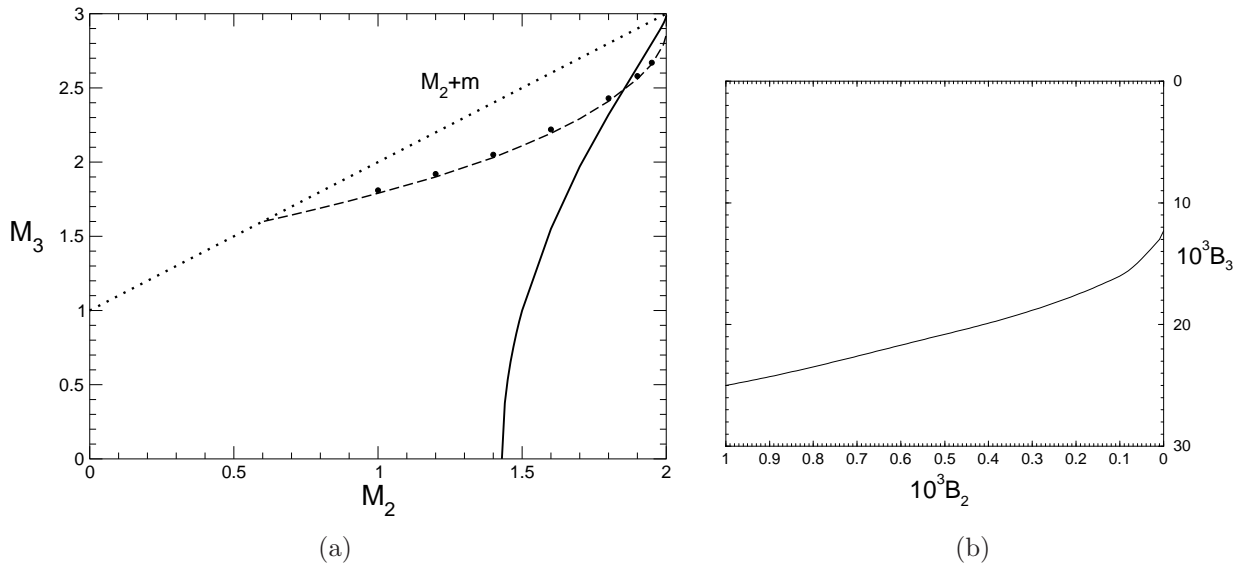


Figure 3: (a) Three-body bound state mass M_3 versus the two-body one M_2 (solid line). Dotted line represents the dissociation limit. Results obtained with integration limits (8) are in dash line. Bold dots are taken from [15]. (b) Zoom of the two-body zero binding limit region ($M_2 \rightarrow 2m, B_2 = 2m - M_2 \rightarrow 0$) corresponding to the solid line only.

three-body bound state mass M_3 as a function of the two-body one M_2 (solid line) together with the dissociation limit $M_3 = M_2 + m$ (dotted line). The two-body zero binding limit $B_2 = 2m - M_2 \rightarrow 0$ is magnified in fig. 3b. In this limit the three-boson system has a binding energy $B_3^{(c)} \approx 0.012$.

When M_2 decreases, the three-body mass M_3 decreases very quickly and vanishes at the two-body mass value $M_2 = M_2^{(c)} \approx 1.43$. Whereas the meaning of collapse as used in the Thomas paper [5] implies unbounded nonrelativistic binding energies and cannot be used here, the zero bound state mass $M_3 = 0$ constitutes its relativistic counterpart. Indeed, for two-body masses below the critical value $M_2^{(c)}$, the three-body system no longer exists.

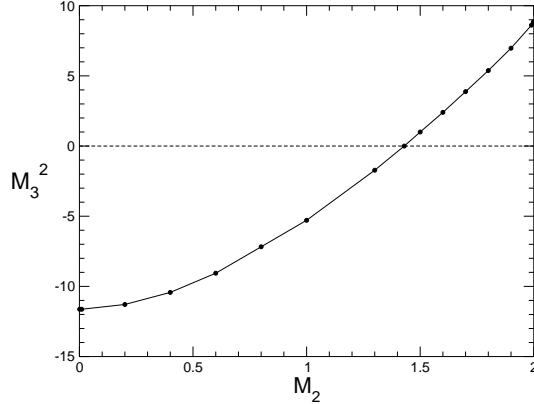


Figure 4: Three-body bound state mass squared M_3^2 versus M_2 .

The results corresponding to integration limits (8) are included in fig. 3a (dash line) for comparison. Values given in [13] were not fully converged. They have been corrected in [15] and are indicated by dots. In both cases the repulsive relativistic effects produce a natural cutoff in equation (6), leading to a finite spectrum and – in the Thomas sense – an absence of collapse, like it was already found in [1]. However, solid and dash curves strongly differ from each other, even in the zero binding limit.

We would like to remark that for $M_2 \leq M_2^{(c)}$, equation (6) possesses square integrable solutions with negative values of M_3^2 . They have no physical meaning but M_3^2 remains finite in all the two-body mass range $M_2 \in [0, 2]$. The results of M_3^2 are given in figure 4. When $M_2 \rightarrow 0$, M_3^2 tends to ≈ -11.6 .

It is also worth noticing that the critical value of the two-body bound state mass $M_2^{(c)}$ as well as the three-body binding energy $B_3^{(c)}$ are universal quantities for bosonic systems. $M_2^{(c)} = 1.43 m$ represents the maximal two-body binding energy $B_2 = 2m - M_2^{(c)} = 0.57 m$ compatible with the existence of 3-boson bound states with mass $M_3 = 0$ ($B_3 = 3m$). $B_3^{(c)} = 0.012 m$ represents the minimal binding energy that a three-boson system can have when two-body binding energy $B_2 = 0$ ($M_2 = 2m$).

3 Two-fermion system with Yukawa interaction

3.1 States with $J = 0$

So far we have considered the behavior of the three-boson relativistic bound system and its critical stability depending on the two-body binding energy. The conclusion are valid for the zero-range interactions, considered as input for the two-body sector, and we have supposed that the particles were spinles.

Now we will study a system of two fermions – spin 1/2 particles – with more sophisticated interaction, resulting from spinless mesons exchange with mass μ . This model traces back to the very origin of the nuclear forces theory proposed by Yukawa. The interaction Lagrangian

reads:

$$\mathcal{L}^{int} = g \bar{\psi} \psi \phi$$

Let us consider first the case of zero total angular momentum $J = 0$. We denote the fermion momenta as \vec{k}_1, \vec{k}_2 . It is convenient to analyze the wave function in the reference frame where $\vec{k}_1 = \vec{k}_2 = 0$. Then the two-fermion wave function depends on the relative momentum $\vec{k} = \vec{k}_1 = -\vec{k}_2$ and on the spin projections of each fermion $\sigma_1, \sigma_2 = \pm 1/2$. Relative to the spin projections, it is a 2×2 matrix which has the following general form [16]:

$$\psi(\vec{k}, \vec{n}) = \frac{1}{\sqrt{2}} \left(f_1 + \frac{i\vec{\sigma} \cdot [\vec{k} \times \vec{n}]}{\sin \theta} f_2 \right), \quad (9)$$

where $\vec{\sigma}$ are the Pauli matrices, $\vec{n} = \vec{\omega}/\omega_0$ and θ is the angle between \vec{k} and \vec{n} . One cannot construct any other independent structures in addition to those appearing in (9). Therefore the 2×2 matrix $\psi(\vec{k}, \vec{n})$ contains only two independent matrix elements or, correspondingly, it is determined by the two coefficients f_1, f_2 of the independent structures. The normalization condition has the form:

$$\frac{m}{(2\pi)^3} \int (f_1^2 + f_2^2) \frac{d^3 k}{\varepsilon_k} = 1, \quad \varepsilon_k = \sqrt{m^2 + k^2}.$$

The equation for the wave function is reduced to a system of two coupled equations for $f_{1,2}$:

$$\begin{aligned} & \left[4(k^2 + m^2) - M^2 \right] f_1(k, \theta) \\ &= -\frac{m^2}{2\pi^3} \int [K_{11}(k, \theta; k', \theta') f_1(k', \theta') + K_{12}(k, \theta; k', \theta') f_2(k', \theta')] \frac{d^3 k'}{\varepsilon_{k'}}, \\ & \left[4(k^2 + m^2) - M^2 \right] f_2(k, \theta) \\ &= -\frac{m^2}{2\pi^3} \int [K_{21}(k, \theta; k', \theta') f_1(k', \theta') + K_{22}(k, \theta; k', \theta') f_2(k', \theta')] \frac{d^3 k'}{\varepsilon_{k'}} \end{aligned} \quad (10)$$

with the kernels:

$$K_{ij} = \int_0^{2\pi} \frac{\kappa_{ij}}{(K^2 + \mu^2) m^2 \varepsilon_k \varepsilon_{k'}} \frac{d\phi'}{2\pi}, \quad (11)$$

where

$$\begin{aligned} K^2 &= k^2 + k'^2 - 2kk' \left(1 + \frac{(\varepsilon_k - \varepsilon_{k'})^2}{2\varepsilon_k \varepsilon_{k'}} \right) \cos \theta \cos \theta' - 2kk' \sin \theta \sin \theta' \cos \phi' \\ &+ \left(\varepsilon_k^2 + \varepsilon_{k'}^2 - \frac{1}{2} M^2 \right) \left| \frac{k \cos \theta}{\varepsilon_k} - \frac{k' \cos \theta'}{\varepsilon_{k'}} \right| \end{aligned} \quad (12)$$

Here ϕ' is the azimuthal angle between \vec{k} and \vec{k}' in the plane orthogonal to \vec{n} and

$$\cos \theta = \cos \vec{n} \cdot \vec{k} / k, \quad \cos \theta' = \cos \vec{n} \cdot \vec{k}' / k'.$$

The explicit expressions for κ_{ij} is given by [16, 17]:

$$\begin{aligned}
\kappa_{11} &= -\alpha\pi \left[2k^2k'^2 + 3k^2m^2 + 3k'^2m^2 + 4m^4 - 2kk'\varepsilon_k\varepsilon_{k'} \cos\theta \cos\theta' \right. \\
&\quad \left. - kk'(k^2 + k'^2 + 2m^2) \sin\theta \sin\theta' \cos\phi' \right], \\
\kappa_{12} &= -\alpha\pi m(k^2 - k'^2)(k' \sin\theta' + k \sin\theta \cos\phi'), \\
\kappa_{21} &= -\alpha\pi m(k'^2 - k^2)(k \sin\theta + k' \sin\theta' \cos\phi'), \\
\kappa_{22} &= -\alpha\pi \left[(2k^2k'^2 + 3k^2m^2 + 3k'^2m^2 + 4m^4 - 2kk'\varepsilon_k\varepsilon_{k'} \cos\theta \cos\theta') \cos\phi' \right. \\
&\quad \left. - kk'(k^2 + k'^2 + 2m^2) \sin\theta \sin\theta' \right], \tag{13}
\end{aligned}$$

where we denote $\alpha = g^2/(4\pi)$.

3.2 Asymptotical behavior of the kernels

The r.h.-sides of equations (10) contain the integrals over k' in infinite limits. The existence of a finite solution depends critically on the behavior of the kernels K_{ij} at large momenta. For the kernels (13) determining the $J = 0$ state, we get the following leading terms:

$$\begin{aligned}
K_{11} &\propto \begin{cases} \frac{1}{k}, & \text{if } k \rightarrow \infty, k' \text{ fixed} \\ \frac{1}{k'}, & \text{if } k' \rightarrow \infty, k \text{ fixed} \end{cases} \\
K_{12} &\propto \begin{cases} \frac{1}{k}, & \text{if } k \rightarrow \infty, k' \text{ fixed} \\ c_{12}, & \text{if } k' \rightarrow \infty, k \text{ fixed} \end{cases} \\
K_{21} &\propto \begin{cases} c_{21} = c_{12}, & \text{if } k \rightarrow \infty, k' \text{ fixed} \\ \frac{1}{k'}, & \text{if } k' \rightarrow \infty, k \text{ fixed} \end{cases} \\
K_{22} &= \begin{cases} c_{22}, & \text{if } k \rightarrow \infty, k' \text{ fixed}, \\ c'_{22}, & \text{if } k' \rightarrow \infty, k \text{ fixed} \end{cases} \tag{14}
\end{aligned}$$

In the above equations the coefficients $c_{12} = c_{21}$, c_{22} and c'_{22} depend on θ, θ' . The coefficients c_{22}, c'_{22} are positive:

$$c_{22} = \frac{\alpha\pi \sin\theta \sin\theta'}{m(1 + \cos\theta)(\varepsilon_{k'} - k' \cos\theta')} > 0, \tag{15}$$

and c'_{22} is obtained from c_{22} by the replacement $k' \rightarrow k, \theta \leftrightarrow \theta'$.

Note that the second iteration of the kernel K_{11} converges at $k' \rightarrow \infty$:

$$\int^L K_{11} G_0 K_{11} \frac{d^3 k'}{\varepsilon_{k'}} \propto \int^L \frac{1}{k'} \frac{1}{k'^2} \frac{1}{k'} \frac{k'^2 dk'}{k'} = \int^L \frac{dk'}{k'^3} \propto \text{const.}$$

Here $G_0 \propto 1/k'^2$ is the intermediate propagator. The integrals

$$\int K_{21} G_0 K_{11} d^3 k' / \varepsilon_{k'} \quad , \quad \int K_{11} G_0 K_{12} d^3 k' / \varepsilon_{k'}$$

are also convergent, whereas the the second iteration of the kernel K_{22} diverges logarithmically:

$$\int^L K_{22} G_0 K_{22} \frac{d^3 k'}{\varepsilon_{k'}} \propto \int^L \text{const} \frac{1}{k'^2} \text{const} \frac{k'^2 dk'}{k'} = \int^L \frac{dk'}{k'} \propto \log(L).$$

The integrals

$$\int K_{12} G_0 K_{22} d^3 k' / \varepsilon_{k'} \quad , \quad \int K_{22} G_0 K_{21} d^3 k' / \varepsilon_{k'}$$

also diverge logarithmically. This is a manifestation of the logarithmical divergence of the box fermion diagram in LFD.

In the domain where both k, k' tend to infinity, but the ratio $k'/k = \gamma$ is fixed, we find for K_{11} :

$$K_{11} = -\frac{2\pi^2 \alpha'}{m} \begin{cases} \sqrt{\gamma} A_{11}(\theta, \theta', \gamma), & \text{if } \gamma \leq 1 \\ \frac{A_{11}(\theta, \theta', 1/\gamma)}{\sqrt{\gamma}}, & \text{if } \gamma \geq 1 \end{cases} \quad (16)$$

with the function $A_{11}(\theta, \theta', \gamma)$:

$$A_{11}(\theta, \theta', \gamma) = \frac{1}{\sqrt{\gamma}} \int_0^{2\pi} \frac{d\phi}{2\pi} \frac{2\gamma(1 - \cos \theta \cos \theta') - (1 + \gamma^2) \sin \theta \sin \theta' \cos \phi}{(1 + \gamma^2)(1 + |\cos \theta - \cos \theta'| - \cos \theta \cos \theta') - 2\gamma \sin \theta \sin \theta' \cos \phi}, \quad (17)$$

where we set $\alpha' = \alpha/(2m\pi)$. In eq. (16) we extracted for convenience the factor $\sqrt{\gamma}$. In the limit $\gamma \rightarrow 0$ A_{11} has the behavior $A_{11}(\theta, \theta', \gamma) \propto \sqrt{\gamma}$.

In the same domain, the kernel K_{22} also has asymptotic (16) with the corresponding function A_{22} given by:

$$A_{22}(\theta, \theta', \gamma) = -\frac{1}{\sqrt{\gamma}} \int_0^{2\pi} \frac{d\phi}{2\pi} \frac{(1 + \gamma^2) \sin \theta \sin \theta' - 2\gamma(1 - \cos \theta \cos \theta') \cos \phi}{(1 + \gamma^2)(1 + |\cos \theta - \cos \theta'| - \cos \theta \cos \theta') - 2\gamma \sin \theta \sin \theta' \cos \phi}. \quad (18)$$

In the limit $\gamma \rightarrow 0$ this function has the behavior $A_{22}(\theta, \theta', \gamma) \propto -1/\sqrt{\gamma}$.

Comparing the above formulas, we see that the dominating kernel is K_{22} . It does not decreases in any direction of the (k, k') plane, whereas in the domain $k \rightarrow \infty$, k' fixed, and vice versa, the kernels K_{11} decrease. In the domain $k'/k = \gamma$ fixed, $k \rightarrow \infty$, both kernels do not decrease, but K_{22} is proportional to the unbounded function A_{22} .

3.3 The cutoff dependence of the binding energy

We are now in position to investigate the stability of the bound states. To disentangle the two different sources of collapse, we will first consider the one channel problem for the component f_1 with the kernel K_{11} . We remove the second equation from (10) and deal with the single equation:

$$[4(\vec{k}^2 + m^2) - M^2] f_1(k, z) = -\frac{m^2}{2\pi^3} \int K_{11}(k, z; k', z') f_1(k') \frac{d^3 k'}{\varepsilon_{k'}}. \quad (19)$$

Our further analysis is based on the collpas condition found by Smirnov [18]. It is obtained by analyzing the asymptotic of eq. (19) with the kernel represented by eq. (16). The solution is searched in the form

$$f_1(k, z) \propto \frac{f(z)}{k^{2+\beta}}. \quad (20)$$

In eq. (19) one should make the replacement of variables $k' = \gamma k$ and take the limit $k \rightarrow \infty$. Provided the kernel $K_{11}(k, k' = \text{const})$ decreases like $1/\sqrt{k}$ or faster, one gets:

$$4k^2 \frac{f(z)}{k^{2+\beta}} = -\frac{m^2}{2\pi^3} \int K_{11}(k, z; k\gamma, z') \frac{f(z')}{(k\gamma)^{2+\beta}} \frac{k^3 \gamma^2 d\gamma 2\pi dz'}{k\gamma}.$$

Splitting the integral in two terms:

$$\int_0^\infty \dots d\gamma = \int_0^1 \dots d\gamma + \int_1^\infty \dots d\gamma,$$

making in the second term the substitution $\gamma = 1/\gamma'$ and substituting here the kernel (16), we obtain the equation:

$$f(z) = 2m\alpha' \int_0^1 dz' f(z') \int_0^1 d\gamma \frac{A_{11}(\gamma, z, z')}{\sqrt{\gamma}} \cosh(\beta \log(\gamma)) \quad (21)$$

Using the symmetry relative to $z \rightarrow 1 - z$, we replaced the integral $\int_{-1}^1 \dots dz'$ by $2 \int_0^1 \dots dz'$.

In the above equations we neglected the binding energy, supposing that it is finite. For given α' the equation (21) gives the value of β , determining the wave function asymptotic (20) for the solution with finite energy. The function $\cosh(\beta \log(\gamma))$ in (21) has minimum at $\beta = 0$. When the factor α' in (21) increases, this is compensated by decrease of $\cosh(\beta \log(\gamma))$, so the value of β is approaching to 0. The maximal, critical value of α' is achieved when $\beta = 0$. So, if we solve the eigenvalue equation [18]:

$$\int_0^1 H(z, z') f(z') dz' = \lambda f(z), \quad \text{with} \quad H(z, z') = 2 \int_0^1 \frac{A_{11}(\gamma, z, z')}{\sqrt{\gamma}} d\gamma \quad (22)$$

then the critical value of α' is related to λ as $\alpha'_c = \frac{1}{m\lambda}$, that gives for the coupling constant in the Yukawa model $\alpha = g^2/(4\pi) = 2\pi m\alpha'$ the following critical value:

$$\alpha_c = \frac{2\pi}{\lambda}. \quad (23)$$

Note that if $A_{11}(\gamma, z, z') = A(\gamma)$ does not depend on z, z' , one gets [18]:

$$\alpha'_c = \frac{1}{2m \int_0^1 \frac{A(\gamma)}{\sqrt{\gamma}} d\gamma}. \quad (24)$$

For the potential $V(r) = -\alpha'/r^2$ one can find $A(\gamma) = 1$ and one gets the well known value $\alpha'_c = 1/(4m)$ [2]. In [19] we have estimated $\alpha_c = \pi$ by majorating the kernel A_{11} by $A_{11} = \sqrt{\gamma}$. Substitution of this function A_{11} into eq. (24) reproduces this result.

Solving eq. (22) numerically with the function $A_{11}(\gamma, z, z')$ given by eq. (16), we found the only eigenvalue:

$$\lambda = 1.748$$

that gives by eq. (23):

$$\alpha_c = 3.594 \quad \Longleftrightarrow \quad g_c = \sqrt{4\pi\alpha_c} = 6.720$$

in agreement with our numerical estimations [19].

In the two-channel problem, the kernel dominating in asymptotic is K_{22} . In the case $J = 0$ it is positive and corresponds to repulsion. Because of that, this channel does not lead to any collapse. This repulsion cannot prevent from the collapse in the first channel (for enough large α), since due to coupling between two channels the singular potential in the channel 1 "pumps out" the wave function from the channel 2 into the channel 1. So, in the coupled equations system (10) the situation with the cutoff dependence is the same as for one channel. A similar analysis of what we detailed in the one channel case, provided us the critical value of the coupling constant [19, 17]

$$\alpha_c = 3.723 \quad \Longleftrightarrow \quad g_c = \sqrt{4\pi\alpha_c} = 6.840 \quad (25)$$

The critical stability of the Yukawa model has been also considered in the framework of the Bethe-Salpeter equation [20]. By using the methods developed in the previous section we have found [21, 22, 23] similar results of what we have obtained in the Light-Front dynamics. There very existence of a critical coupling constant for the $J=0$ state was confirmed, although with slightly different numerical value:

$$\alpha_c = \pi \quad \Longleftrightarrow \quad g_c = 2\pi \quad (26)$$

to be compared with (25).

3.4 States with $J = 1$

In general, the wave function of the $J = 1$ state is determined by six independent structures [24]. It turns out that the following operator commutes with the kernel:

$$A^2 = (\vec{n} \cdot \vec{J})^2. \quad (27)$$

Since A^2 is a scalar, it commutes also with \vec{J} . Therefore, in addition to J, J_z , the solutions are labeled by a :

$$A^2 \vec{\psi}^a(\vec{k}, \vec{n}) = a^2 \vec{\psi}^a(\vec{k}, \vec{n}). \quad (28)$$

Though the wave function for $J = 1$ is determined by six components, the equation system is split in two subsystems with $a = 0$ and $a = 1$, containing 2 and 4 equations respectively [16].

The function $\vec{\psi}^0$ corresponding to $J = 1, a = 0$ has the following general decomposition:

$$\vec{\psi}^0(\vec{k}, \vec{n}) = \sqrt{\frac{3}{2}} \left\{ g_1^{(0)} \vec{\sigma} \cdot \hat{\vec{k}} + g_2^{(0)} \frac{\vec{\sigma} \cdot (\hat{\vec{k}} \cos \theta - \vec{n})}{\sin \theta} \right\} \vec{n}, \quad (29)$$

where $\hat{\vec{k}}$ denotes the unit vector $\hat{\vec{k}} = \vec{k}/k$. Since it corresponds to $J^\pi = 1^+$, it is a pseudovector. Since \vec{n} is a true vector ($J^\pi = 1^-$), it should be multiplied by a pseudoscalar. We can construct two pseudoscalars only: $\vec{\sigma} \cdot \hat{\vec{k}}$ and $\vec{\sigma} \cdot \hat{\vec{n}}$, what gives two terms. The particular structures in (29) are constructed in such a way to be orthogonal and normalized to 1.

The function $\vec{\psi}^1$ satisfies the orthogonality condition $\vec{\psi}^1 \cdot \vec{n} = 0$. To satisfy this condition, it is convenient to introduce the vectors orthogonal to \vec{n} :

$$\hat{k}_\perp = \frac{\hat{k} - \cos \theta \vec{n}}{\sin \theta}, \quad \vec{\sigma}_\perp = \vec{\sigma} - (\vec{n} \cdot \vec{\sigma}) \vec{n}.$$

Then the function $\vec{\psi}^1$ obtains the following general form:

$$\vec{\psi}^1(\vec{k}, \vec{n}) = g_1^{(1)} \frac{\sqrt{3}}{2} \vec{\sigma}_\perp + g_2^{(1)} \frac{\sqrt{3}}{2} \left(2\hat{k}_\perp (\hat{k}_\perp \cdot \vec{\sigma}_\perp) - \vec{\sigma}_\perp \right) + g_3^{(1)} \sqrt{\frac{3}{2}} \hat{k}_\perp (\vec{\sigma} \cdot \vec{n}) + g_4^{(1)} \sqrt{\frac{3}{2}} i [\hat{k} \times \vec{n}] \quad (30)$$

In summary, the system of six equations for the $J=1$ state is split in two subsystems: two equations for $a = 0$ and four for $a = 1$. The subsystem for $a = 0$ has the same structure than (10) with different kernels $K_{ij}^{(J=1)}$. The asymptotic of the kernel $K_{22}^{(J=1)}$ is the same than $-K_{22}^{(J=0)}$: it is negative and corresponds to attraction. The integral (22) for the kernel $H(z, z')$ with the function A_{22} given by (18) diverges logarithmically. Therefore it results in a collapse for any value of the coupling constant. This result coincides with conclusion of the paper [25].

3.5 Numerical results

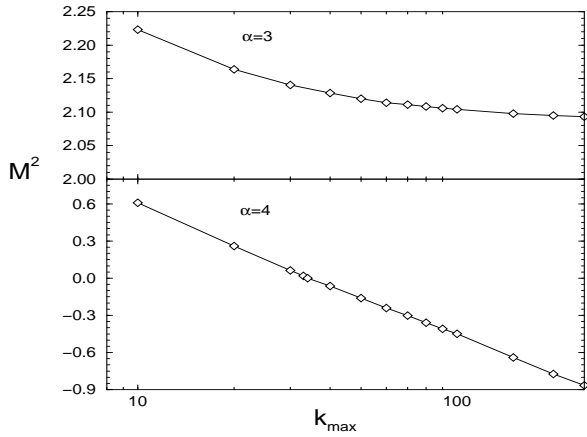


Figure 5: Cutoff dependence of the binding energy in the $J = 0$ state, in the one-channel problem (f_1), for two fixed values of the coupling constant below and above the critical value.

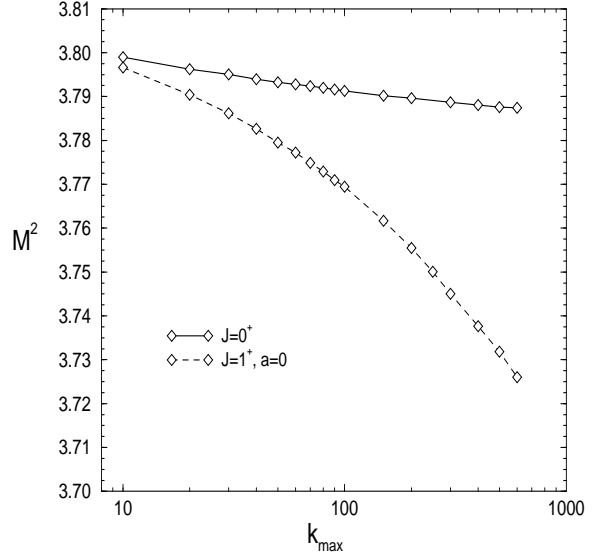


Figure 6: Cutoff dependence of the binding energy, for $J = 0$ and $J = 1, J_z = 0$ states, in full (two-channel) problem, for $\alpha = 1.184$.

The preceding analysis are confirmed by several numerical calculations. In all what follows, the constituent masses were taken equal to $m=1$ and the mass of the exchanged scalar $\mu=0.25$.

Let us first present the results given by the one channel problem: a single equation for f_1 with kernel K_{11} in the $J = 0$ case. We have plotted in figure 5 the mass square M^2 of the two fermion system as a function of the cutoff k_{max} for two fixed values of the coupling constant below and above the critical value. In our calculations the cutoff appears directly as the maximum value k_{max} up to which the integrals in (10) are performed. One can see two dramatically different behaviors depending on the value of the coupling constant α . For $\alpha = 3$, i.e. $\alpha < \alpha_c = 3.594$, the result is convergent. For $\alpha = 4$, i.e. $\alpha > \alpha_c$, the result is clearly divergent. M^2 decreases logarithmically as a function of k_{max} and becomes even negative. This property is due only to the large k behavior of K_{11} . Though the negative values of M^2 which appear in fig. 5 are physically meaningless, they are formally allowed by the equations (10). The first degree of M does not enter neither in the equation nor in the kernel, and M^2 crosses zero without any singularity. The value of the critical α does not depend on the exchange mass μ . For $\mu \ll m$, e.g. $\mu \approx 0.25$, its existence is not relevant in describing physical states since any solution with positive M^2 , stable relative to cutoff, corresponds to $\alpha < \alpha_c$. For $\mu \sim m$ one can reach the critical α for positive, though small values of M^2 .

We consider now the full Yukawa problem as given by the two coupled equations (10). In figure 6 are displayed the variations of M^2 for $J = 0$ and $J = 1, J_z = 0$ states as a function of the cutoff k_{max} . The value of the coupling constant for both J is $\alpha_c = 1.184$, the same that in fig. 2 of [25], below the critical value. Our numerical values are in agreement with the results for the cutoff $\Lambda \leq 100$ presented in this figure [25], but our calculation at larger k_{max} leads to different conclusion for the $J = 0$ state. We first notice a qualitatively different behavior of the two states. In what concerns $J = 0$, the numerical results become more flat when k_{max} increases, – with less than a 0.5% variation in M^2 when changing k_{max} between $k_{max}=10$ and 300. This strongly suggests a convergence. We thus conclude to the stability of the state with $J = 0$, as expected from our analysis in sect. 3.3.

On the contrary, for $J = 1, J_z = 0$ the value of $M^2(k_{max})$ continues to decrease faster than logarithmically and indicates, – as found in [25], – a collapse. As mentioned above, the asymptotic of the $K_{22}^{(J=1)}$ kernel is the same as the $K_{22}^{(J=0)}$ one but with an opposite sign, i.e. it is attractive, what leads to instability for any value of α . The same result was found when solving the $J = 0$ equations with the opposite sign of $K_{22}^{(J=0)}$.

3.6 Positronium

We applied our method to the positronium system in the $J = 0^-$, a bound state of electron and positron which exists in nature. We consider this important application in more detail.

The wave function is again determined by two components and has the form (9). The negative parity of the state comes from the intrinsic positron parity so that the corresponding kernels are those of the $J^\pi = 0^+$ two-fermion system. They were derived, for the Feynman gauge in [16] (eqs. (A8) in appendix A). They have the form (11) with the following values κ_{ij} instead of eqs. (13) for the scalar case:

$$\begin{aligned}\kappa_{11} &= -2\pi\alpha(4k^2k'^2 + 3m^2(k^2 + k'^2) + 2m^4) \\ \kappa_{12} &= 2\pi\alpha mk'(k^2 - k'^2) \sin \theta' \\ \kappa_{21} &= -2\pi\alpha mk(k^2 - k'^2) \sin \theta\end{aligned}\tag{31}$$

$$\kappa_{22} = -2\pi\alpha[kk'(k^2 + k'^2 + 2m^2) \sin\theta \sin\theta' + 2\epsilon_k\epsilon_{k'}(\epsilon_k\epsilon_{k'} + kk' \cos\theta \cos\theta') \cos\phi']$$

Following sect. 3.2, we substitute $k' = \gamma k$ and take the limit $k \rightarrow \infty$. The non-diagonal kernels tend to zero, whereas for K_{11} and K_{22} we reproduce (16) with the following kernels $A(\theta, \theta', \gamma)$:

$$A_{11}(\theta, \theta', \gamma) = 8\sqrt{\gamma} \int_0^{2\pi} \frac{d\phi}{2\pi} \frac{1}{(1 + \gamma^2)(1 + |\cos\theta - \cos\theta'| - \cos\theta \cos\theta') - 2\gamma \sin\theta \sin\theta' \cos\phi}, \quad (32)$$

$$A_{22}(\theta, \theta', \gamma) = \frac{2}{\sqrt{\gamma}} \int_0^{2\pi} \frac{d\phi}{2\pi} \frac{(1 + \gamma^2) \sin\theta \sin\theta' + 2\gamma(1 + \cos\theta \cos\theta') \cos\phi}{(1 + \gamma^2)(1 + |\cos\theta - \cos\theta'| - \cos\theta \cos\theta') - 2\gamma \sin\theta \sin\theta' \cos\phi}, \quad (33)$$

where we denote $\alpha' = \alpha/(2m\pi)$.

At $\gamma \rightarrow 0$ A_{22} has the behavior: $A_{22}(\theta, \theta', \gamma) \propto +1/\sqrt{\gamma}$ (compare with $A_{22}(\theta, \theta', \gamma) \propto -1/\sqrt{\gamma}$ in eq. (18) for Yukawa model).

As discussed at the end of sect. 3.3, the behavior $A_{22}(\theta, \theta', \gamma) \propto -1/\sqrt{\gamma}$ corresponds to repulsion, hence for positronium with $A_{22}(\theta, \theta', \gamma) \propto +1/\sqrt{\gamma}$ we have attraction. The integral (22) diverges and the spectrum is unbounded from below.

This conclusion is confirmed by numerical calculations. In table 1 are presented the values of the coupling constant α as a function of the sharp cut-off k_{max} and for a fixed binding energy $B = 0.0225$. The dependence is very slow – 0.3% variation for $k_{max} \in [10, 300]$ – but it actually corresponds to a logarithmic divergence of $\alpha(k_{max})$ as it can be seen in fig. 7. The origin of

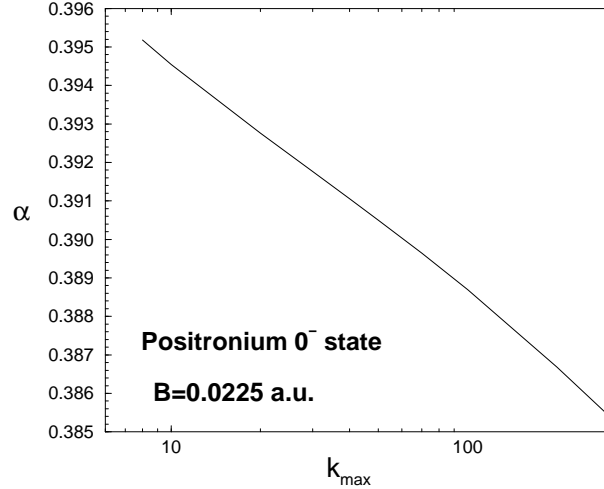


Figure 7: Coupling constant α as a function of the sharp cut-off k_{max} for the $J = 0^-$ positronium state with binding energy $B = 0.0225$ a.u.

this instability is the coupling to the second component, whose kernel matrix element κ_{22} has an attractive, constant asymptotic limit. If one removes this component – which has a very small contribution in norm – calculations become stable and give for $\alpha_{NR} = 0.30$ the value $\alpha_{LFD} = 0.3975$. We should emphasize that as one can see from fig. 7 and from the table 1,

Table 1: Coupling constant α as a function of the sharp cut-off k_{max} for the $J = 0^-$ positronium state with binding energy $B = 0.0225$ a.u.

k_{max}	10	20	30	40	50	70	100	200	300
α	0.3945	0.3928	0.3918	0.3911	0.3905	0.3896	0.3887	0.3867	0.3854

the development of this instability vs. k_{max} is very slow. The value $k_{max} = 300$ (in units of electron masses) is very large. At this momentum the contributions having other origin (beyond QED), can make influence and change the behavior of the binding energy vs. k_{max} .

Let us now consider also another gauge - the so called light-cone gauge [26] - which is often used in the light-front dynamics calculations. In the explicitly covariant version of LFD, the photon propagator in the light-cone gauge, is obtained from the Feynman one by the replacement (see eq. (2.65) from [10]):

$$-g_{\mu\nu} \rightarrow -g_{\mu\nu} + \frac{\omega_\mu k_\nu + \omega_\nu k_\mu}{\omega \cdot k} \quad (34)$$

The behavior $1/\omega \cdot k \sim 1/x$ is singular and should be regularized [26]. There are two graphs corresponding to the photon exchange which differ from each other by the order of vertices in the light-front time, see e.g. fig. 3 from [16]. The value of the momentum k transferred by photon is different in these LF graphs, see eq. (14) from [16]. By performing the calculations, we have found that the second term in (34) gives additional contributions to eqs. (32) and (33) which turns into:

$$A_{11}(\theta, \theta', \gamma) = \int_0^{2\pi} \frac{d\phi}{2\pi D} \left[8\sqrt{\gamma} + \frac{4(1 + \gamma^2) \sin \theta \sin \theta' \cos \phi}{\sqrt{\gamma} |\cos \theta - \cos \theta'|} \right] \quad (35)$$

$$A_{22}(\theta, \theta', \gamma) = \int_0^{2\pi} \frac{d\phi}{2\pi D} \left[\frac{2}{\sqrt{\gamma}} [(1 + \gamma^2) \sin \theta \sin \theta' + 2\gamma(1 + \cos \theta \cos \theta') \cos \phi] + \frac{4(1 + \gamma^2) \sin \theta \sin \theta'}{\sqrt{\gamma} |\cos \theta - \cos \theta'|} \right] \quad (36)$$

The singularity $\sim 1/|\cos \theta - \cos \theta'|$ appears from $1/x$ in (34) and, as mentioned, it should be regularized. In the limit $\gamma \rightarrow 0$, the extra contribution $\sim 1/\sqrt{\gamma}$ in $A_{11}(\theta, \theta', \gamma)$ is smoothen due to the integration over ϕ , whereas it does not change the behavior of $A_{22}(\theta, \theta', \gamma)$ which remains of the form $A_{22}(\theta, \theta', \gamma) \propto +1/\sqrt{\gamma}$. As explained above, this corresponds to a spectrum unbounded from below. This is manifested by an unbounded increasing of the binding energy B as a function of the cutoff k_{max} or by a decreasing - down to zero - of the coupling constant α for a fixed value of the binding energy, as it is shown in fig. 7 and in the table 1. We would like to again that this dependence on k_{max} , fatal for the very existence of stable bound states, is very weak and so not at all easy to find its evidence in numerical calculations, specially when using non-uniform mappings.

Due to this very slow k_{max} -dependence we have fixed the cut-off to an arbitrary value $k_{max} = 10$ and considered the case $\alpha = 3$. The non relativistic binding energy is $B = 0.0225$ and we found, for the ladder LFD in the Feynman gauge [16], a value $B_{LFD} = 0.0132$, that is a strong repulsive effect. This repulsion, observed in most of the kernels examined both for

bosons and fermions, however contradicts the leading order QED corrections [27]

$$B_{QED} = \frac{\alpha^2}{4} \left[1 + \frac{21}{16} \alpha^2 + o(\alpha^4) \right] \approx 0.02516,$$

which are attractive. This indicates that the ladder light-front kernel, in the Feynman gauge, is unable to predict even the sign for the relativistic corrections of such a genuine system. It remains to see if this failure is a consequence of the relative simplicity of the ladder sum or it has other reason.

4 Conclusions

In the relativistic framework of Light-Front Dynamics, we have studied the critical stability of three equal-mass bosons, interacting via zero-range forces and the two-fermion system interacting via ladder scalar, pseudoscalar and vector exchanges.

The three equal-mass bosons interact via zero-range forces constrained to provide finite two-body mass M_2 . We have found that the three-body bound state exists for two-body mass values in the range $M_2^{(c)} = 1.43m \leq M_2 \leq 2m$. At the zero two-body binding limit, the three-body binding energy is $B_3^{(c)} \approx 0.012m$ and represent the minimal binding energy for a three bosons system with contact interactions. The Thomas collapse is avoided in the sense that three-body mass M_3 is finite, in agreement with [1, 13].

However, another kind of catastrophe happens. Although removing infinite binding energies, the relativistic dynamics generates zero three-body mass M_3 at a critical value $M_2 = M_2^{(c)}$. For stronger interaction, i.e. when $0 \leq M_2 < M_2^{(c)}$, there are no physical solutions of the Light-Front equations with real value of M_3 . In this domain, M_3^2 becomes negative.

If in the non-relativistic dynamics the system collapses when its binding energy tends to $-\infty$, in the relativistic approach the system does not exist when its mass squared is negative. This fact can be interpreted as the relativistic counterpart of the non-relativistic Thomas collapse.

We extended this study to two-fermion system interacting by exchange of scalar pseudo scalar and vector particles. In [16] we have separately examined the different types of these couplings and found very different behaviors concerning the stability of the solutions themselves and their relation with the corresponding non relativistic reductions.

In particular, the scalar coupling (Yukawa model) is found to be stable without any kernel regularization for the $J^\pi = 0^+$ state and coupling constants below some critical value $\alpha < \alpha_c = 3.72$. For values above α_c the system collapses. For $J^\pi = 1^+$ state the solution is unstable. The comparison with the non relativistic solutions shows always repulsive effects.

Electromagnetic coupling presents the stronger anomalies. It has been applied to positronium 0^+ state. It is found to be unstable and, once regularized by means of sharp cut-off, the ladder approximation in the Feynman gauge gives relativistic corrections of opposite sign compared to QED perturbative results. This failure shows, probably, the poorness of the ladder approximation in one of the rare cases in which it can be confronted to experimental results.

As a final remarks, we would like to emphasize again that, as it was first pointed out in [1], the relativistic dynamics allows to exist, in principle, systems which would not exist in

the non-relativistic framework. Their existence is determined by the properties and strength of relativistic interaction and we denote this fact by "critical stability". The pioneering work of Pierre Noyes [1] opened thus a fruitful and interesting field in the theory of few-body systems.

References

- [1] James V. Lindesay and H. Pierre Noyes, *Zero range scattering theory II. Minimal relativistic three-particle equations and the Efimov effect*, Preprint SLAC-PUB-2932(rev.), 1986.
- [2] L.D. Landau, E.M. Lifshits, *Quantum mechanics*, Pergamon press, 1965.
- [3] G.E. Brown, A.D. Jackson, *The nucleon-nucleon interaction*, North-Holland, Amsterdam, 1976.
- [4] Y.N. Demkov, V.N. Ostrovskii, *Zero-range potentials and their applications in atomic physics*, Plenum Press, New-York 1988.
- [5] L.H. Thomas, *Phys. Rev.* **47** (1935) 903.
- [6] S. K. Adhikari, T. Frederico, I.D. Goldman, *Phys. Rev. Lett.* **74** (1995) 487; T. Frederico, L. Tomio, A. Delfino, A.E.A. Amorim, *Phys. Rev.* **A60** (1999) R9.
- [7] D.V. Fedorov, A.S. Jensen, *Phys. Rev.* **A63** (2001) 063608; *Nucl. Phys.* **A697** (2002) 783.
- [8] M. Mangin-Brinet, J. Carbonell, *Phys. Lett.* **B474**, (2000) 237
- [9] J. Carbonell, V.A. Karmanov, *Phys. Rev.* **C67** (2003) 037001.
- [10] J. Carbonell, B. Desplanques, V.A. Karmanov, J.-F. Mathiot, *Phys. Reports*, **300** (1998) 215.
- [11] S.J. Brodsky, H.-C. Pauli, S.S. Pinsky, *Phys. Reports*, **301** (1998) 299.
- [12] P.A.M. Dirac, *Rev. Mod. Phys.* **21** (1949) 392.
- [13] T. Frederico, *Phys. Lett.* **B282** (1992) 409.
- [14] B.L.G. Bakker, L.A. Kondratyuk, M.V. Terentyev, *Nucl. Phys.* **B158** (1979) 497.
- [15] W.R.B. de Araujo, J.P.B.C. de Melo, T. Frederico, *Phys. Rev.* **C52** (1995) 2733.
- [16] M. Mangin-Brinet, J. Carbonell, V.A. Karmanov, *Phys. Rev.* **C68** (2003) 055203.
- [17] M. Mangin-Brinet, J. Carbonell, V.A. Karmanov, *Phys. Rev.* **D64** (2001) 125005.
- [18] A.V. Smirnov, private communication of Feb. 20, 2001.
- [19] M. Mangin-Brinet, J. Carbonell, V.A. Karmanov, *Phys. Rev.* **D64** (2001) 027701.
- [20] E. Salpeter, H. Bethe, *Phys. Rev.* **84** (1951) 1232–1242.

- [21] J. Carbonell, V. Karmanov, Eur. Phys. J. **A46** (2010) 387–397.
- [22] J. Carbonell, V. Karmanov, Few-Body Syst. **49** (2011) 205–222.
- [23] J. Carbonell, V.A. Karmanov, F. de Soto, Few-Body Syst. (2013); arXiv:1211.5474
- [24] J. Carbonell and V.A. Karmanov, Nucl. Phys. **A581** (1995) 625.
- [25] St. Glazek, A. Harindranath, S. Pinsky, J. Shigemitsu and K. Wilson, Phys. Rev. **D47** (1993) 1599.
- [26] G.P. Lepage, S.J. Brodsky, Phys. Rev. **D22** (1980) 2157.
- [27] H.A. Bethe and E.E. Salpeter, Quantum Mechanics of one- and two-electron atoms, A Plenum/Roseta Ed., (1977).